

Refined preparation of 1 α ,3-dipyrrolidino-androsta-3,5-diene-17-one, a key intermediate in the exemestane synthesis

Ł. KACZMAREK¹, M. CYBULSKI¹, M. KUBISZEWSKI¹, A. LEŚ^{1,2}

Received February 3, 2012, accepted March 31, 2012

Prof. Andrzej Leś, Pharmaceutical Research Institute, Rydygiera 8, 01-793 Warsaw, Poland
a.les@ifarm.eu

Pharmazie 67: 899–905 (2012)

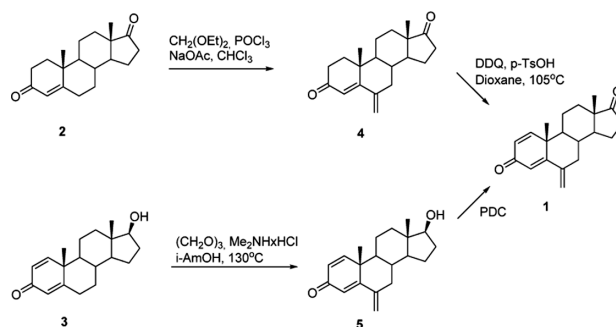
doi: 10.1691/ph.2012.2025

A significant improvement of the patent route for exemestane synthesis has been achieved. The key intermediate 1 α ,3-dipyrrolidino-androsta-3,5-diene-17-one (**7**) was obtained in a good yield and effectively used without further isolation in the next reaction step. The original analytical method for the identification and quantification of the substrate androsta-1,4-diene-3,17-dione (ADD, **6**), intermediate **7** and 1-pyrrolidino-androsta-1,3,5-triene-17-one (**9**) impurity in the reaction mixture was applied. Due to the newly developed process, the economical synthesis of the final pharmaceutical product in a large scale was possible. In addition, the complete NMR characteristics of **7** was described for the first time. The experiments were also analyzed with the theoretical quantum mechanical density functional B3LYP calculations for the energy outputs in model reactions. Based on these studies hypothetical routes of key intermediate (**7**) formation have been suggested. These predictions were consistent with the solutions of kinetic equations fitted to the experimental curves for time-dependence of three components of the reaction mixture.

1. Introduction

Breast cancer is the leading cause of deaths among women (World Cancer Report 2008). One-third of this type of cancer is hormone-dependent and uses estrogen to proliferate (Segaloff 1978). The major source of estrogens in post-menopausal women is enzymatic conversion of circulating androgens. The final step in this process is catalyzed by the aromatase enzyme (Miller 1990). Therefore, the inhibition of this enzyme activity causes tumor regression in post-menopausal women with estrogen-dependent breast cancer (Bajetta et al. 1999). There are two types of aromatase inhibitors. Type II (reversible inhibitors), such as aminoglutethimide, rogletimide, fadrosolol, anastrozole, letrozole and vorozole, act by reversibly binding to the enzyme. Hence ongoing estrogen deprivation needs the continued presence of the drug. This results in enhanced toxicity. Type I aromatase inhibitors, having androstenedione structure, inactivate the enzyme irreversibly. In effect, the renewed estrogen synthesis requires biosynthesis of new enzyme, which results in the reduced toxicity of the drug, since the enzyme inhibition persists after the drug has been removed from the system (Lombardi 2002). One of the Type I aromatase inhibitors is *exemestane* (6-methyleneandrosta-1,4-dione) (**1**) which was launched by the Farmitalia Carlo Erba group (Giudici et al. 1988). Exemestane is significant as the only orally active irreversible steroidal aromatase inhibitor, effectively used in postmenopausal women with advanced breast cancer (Clemett and Lamb 2000). Moreover, it appears that exemestane is also effective for the chemoprevention of breast cancer (Barton 2011).

In general, there are two different routes of obtaining exemestane. The first, applied by Farmitalia Carlo Erba originator, exploits 6-methylation of androstenedione (**2**) according to the general method of Annen et al. (1982) or boldenone (**3**) in Mannich reaction. Then the intermediates **4** or **5** are oxidized

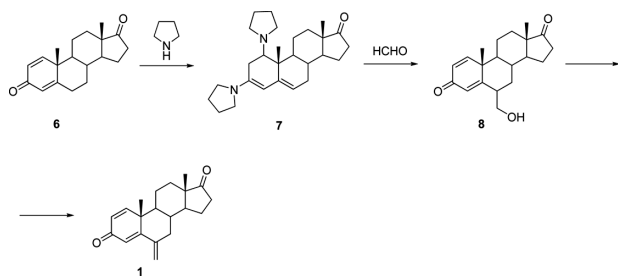


Scheme 1: Two common routes of synthesis of exemestane (**1**)

with DDQ (Buzzetti et al. 1987) or Jones reagent (Longo and Lombardi 1987), respectively (Scheme 1).

The second route, proposed by a German group in 1986, starts from androsta-1,4-diene-3,17-dione (ADD) (**6**). Compound **6** reacts with pyrrolidine to give the corresponding 1,3-dipyrrolidino derivative **7** which readily transforms into 6-(hydroxymethyl)androsta-1,4-dien-3,17-dione (**8**) through stirring with the aqueous formaldehyde (Wagner 1986a, b). The acid-catalyzed dehydration of **8** yields the final exemestane (**1**) (Wagner 1986a, b) (Scheme 2).

The analysis of literature and patent data reveals, that the methods disclosed in patents of Farmitalia group (Buzzetti et al. 1987; Longo and Lombardi 1987) are unfavorable because of toxic and environmentally unsafe reagents (e.g. pyridine chromate, DDQ, POCl₃ or bromine) as well as harsh reaction conditions. From this point of view the exemestane synthesis described in German patents (Wagner 1986a, b) appears to be an advantageous alternative. This method of exemestane synthesis was used formerly (Wojciechowska 2001; Wojciechowska et al. 2004) and follow-



Scheme 2: The exemestane (1) synthesis from ADD (6)

ing some modifications, by Kunnen et al. (2005) from Cedarburg Pharmaceuticals Inc. In both cases the crucial point of the synthesis is the formation of dipyrrolidino derivative **7** followed by its transformation into 6-hydroxymethyl-androstanodienone **8**. In order to develop the technology of exemestane in a pilot scale we examined these reactions, starting from the verification of literature data.

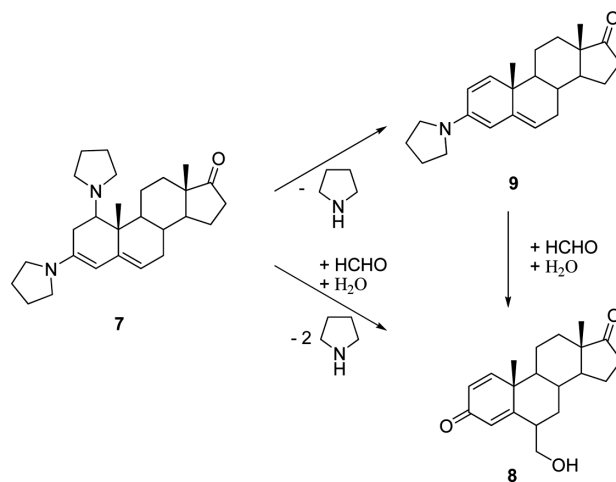
2. Investigations, results and discussion

2.1. Exploration of reaction parameters

According to the procedure described by Wojciechowska et al. (2004), which was based on the previously published procedure from the German patent (Wagner 1986a, b), the compound **7** was slowly formed by refluxing **ADD** (**6**) for 68–80 h in an excess of pyrrolidine (3 mL/g) under inert atmosphere. When the quantity of the starting **6** fell below 10%, the reaction was completed. The reaction could not be controlled by HPLC or TLC techniques because of the instability of **7** during chromatography, so the IR spectroscopy control was applied as a method of choice. The dipyrrolidino adduct **7** was isolated in the yield of 60–70% by removing pyrrolidine excess and crystallization of the residue with methanol.

An attempt to repeat the above procedure revealed that the reaction time increased rapidly when the reaction was scaled up. The consumption of the starting **ADD** exceeding 90% could be reached in 48 h at the 10 g scale, while scaling the reaction up to 60 g of **ADD** prolonged this time to 70 h. In the course of experiment it appeared that the ^1H NMR spectroscopy is an excellent alternative technique for the reaction control (Kubiszewski et al. 2012). Satisfactory separation of the proton signals in the region of chemical shifts δ 4.5–7.5 allowed to calculate the quantity of the compound **7** and the substrate **6** in the reaction mixture. Additionally, the usage of ^1H NMR let us detect the unexpected impurity 1-pyrrolidino-androsta-1,3,5-triene-17-one (**9**) (12–17%) which was not monitored by other authors. We observed that the impurity **9** content, both in the crude reaction mixture and the isolated yellow adduct **7**, strongly depended on the process temperature and increased with the temperature of the reaction. Fortunately, the formation of **9** during the condensation of **ADD** with pyrrolidine was not a problem. It was experimentally confirmed that the compound **9**, like **7**, transformed into the desired intermediate **8** in the next reaction with formaldehyde (Scheme 3). Afterwards, to eliminate the impurity **9** from the process, the reaction temperature was lowered in the successive experiments from about 90 °C (reflux) to 50 °C. It allowed us to obtain the anticipated composition of the crude reaction mixture with 98% conversion to **7**. Moreover, no **9** was detected. It occurred, however, that lower temperature extended the reaction time (up to 120 h). This was technologically not acceptable and obliged us to perform further optimization of the reaction.

In order to shorten the time of the **7** formation in the reaction of **ADD** with pyrrolidine, the second procedure described by

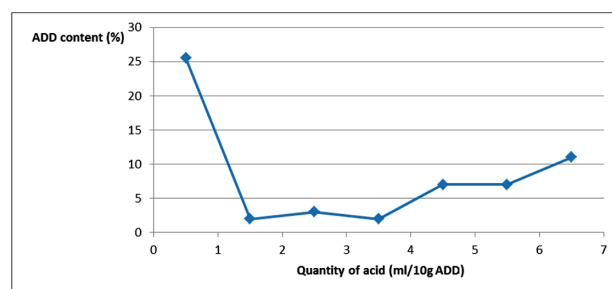
Scheme 3: The transformation of an impurity **9** into the desired intermediate **8**

Cedarburg Pharmaceuticals Inc. (Kunnen 2005) was revisited. Actually, it was confirmed that the addition of a catalytic amount of acetic acid accelerates the reaction in mild temperature conditions (40 °C), but the product cannot be easily isolated - as it was described in the patent application example - from the ethanol medium. Therefore, our next experiments with the acid catalyst were continued without a solvent, in the excess of pyrrolidine. Initially it was found that the acid catalyzed reaction at 50 °C needs only 7 h to yield compound **7**. Then it was demonstrated that the acid catalyzed reaction may be carried out even at ambient temperature under normal atmospheric conditions but its progress depends strongly on the amount of acetic acid added, see Fig. 1.

The acid addition range was established by determining (with NMR spectroscopy) seven single measurement points obtained through adding from 0 to 7 mL of acid per 10 g of **ADD**.

Although the precision of **ADD** content determination is generally moderate, about 1–2 %, we are convinced that the acid range of 0.15–0.30 mL per 1 gram of starting **ADD** is optimal for practical purposes.

At that point the procedure suitable for the reaction carried out in a large scale was achieved. It included the **ADD** (**6**) reaction with an excess of pyrrolidine and without a solvent in the presence of the catalytic amount of the acetic acid. The reaction was carried out in ambient temperature without the inert gas atmosphere for 24 h. This time was sufficient for more than 98% transformation of 100 g **ADD** (**6**). However, there was still a problem of isolating the intermediate **7** from the reaction mixture. Some authors even reported that despite varying reaction conditions, compound **7** could not be isolated (Goerlitzer et al. 2002; Bonnekessel and Görlitzer 2002). In our opinion the essential reason of their failure was the application of column chromatography in the reaction mixture work-up, which led to the arrangement of an estrone derivative instead of **7** purification. It was found

Fig. 1: The **ADD** content as a function of the quantity of acetic acid added (ambient temperature, 24 h)

that in contrary to the described procedures (Kunnen et al. 2005; Wojciechowska et al. 2004), the adduct **7** cannot be obtained in proper yield from a crude reaction mixture by crystallization or precipitation from organic solvents because of a very good solubility in that media. While verifying Cedarburg Pharmaceuticals Inc. work-up procedure (Kunnen et al. 2005) we noticed that the evaporation of the solvent excess, followed by the cooling of the mixture and product filtration, gave the compound **7** with unsatisfactory 60% yield. The second work-up procedure (Wojciechowska 2001) strongly decreased the yield of **7** from *ca.* 100% in crude oily product after the evaporation of reaction mixture to 60% of yellow crystals after crystallization from methanol. The obtained results seemed economically unfavorable. The applicability of other organic solvents as potential crystallization media was studied but no positive results were observed. Although the intermediate **7** was also susceptible to hydrolysis, it appeared that its short contact with water was rather harmless. We found that the key intermediate **7** could be successfully isolated from the reaction mixture by diluting with water, filtering the precipitate and washing with water. The wet precipitate of **7** could not be dried because of its instability during the drying process. The content of **7**, following 120 h of air-drying at ambient temperature, reached the level of 65%, with 18% back-conversion to the starting **ADD (6)**.

Therefore we tested the ability of the wet **7** to react with formalin. It was noticed that the above reaction provided the expected compound **8** with good yield and purity. Our experimental observations led us to the conclusion that crude **7** can be used in the next reaction without an isolation.

At first we examined the reaction of the crude **7**. After the condensation of **ADD** with pyrrolidine the excess of pyrrolidine was evaporated, the slurry just dissolved in dichloromethane and stirred with formalin. This procedure, however, resulted in an unsatisfactory yield of the product **8**. Therefore, we decided to remove the pyrrolidine and its acetate traces by fast washing the dichloromethane solution with water, prior to the reaction with aqueous formaldehyde. This work-up procedure allowed us to achieve the intermediate **8** with high total yield (76–80%) and purity (97.5%) and it also extremely simplified the technological process.

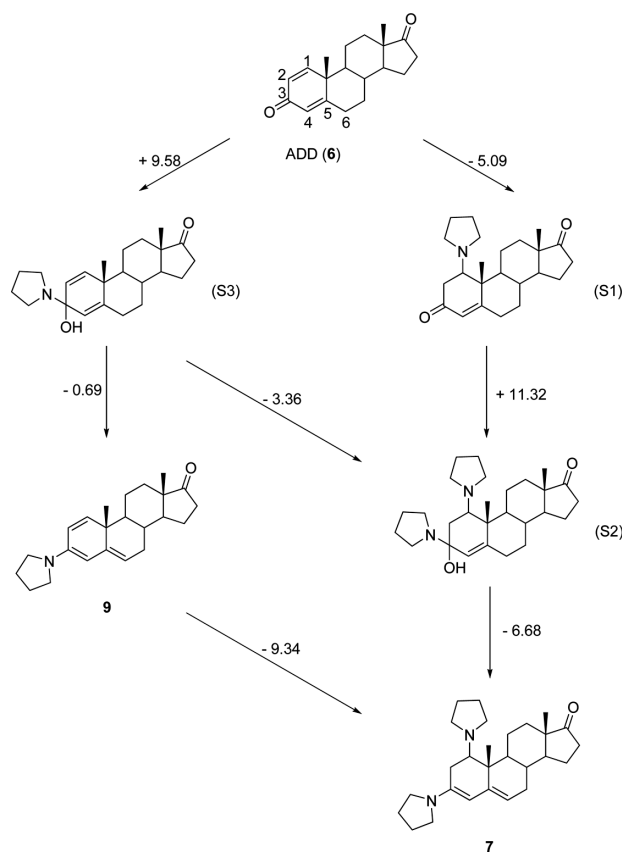
Besides, we managed to obtain a pure compound **7** for analytical purposes. The wet **7**, after the precipitation from water, was dissolved in CDCl_3 and the NMR data was collected after the separation of the organic phase. In this way we reported the first complete NMR characteristics for compound **7** by comparing the calculated results with the experimental data.

To summarize, by sampling of reaction parameters like reaction time, temperature, the amount of the acid catalyst and some details of the work-up procedure in the course of several experiments we have managed to formulate reasonable conditions for **ADD** transformation to **7**. The present technology is considerably improved in comparison to the existing ones and it is the matter of our patent application (Kaczmarek et al. 2010).

2.2. Hypothetical routes of **7** formation

Taking into consideration our observation of the instability of **7** during the studies on various work-up procedures, possible molecular transformation routes of **ADD (6)** to **7** were analyzed (see Scheme 4).

The molecular structures and their molecular energies were calculated with the theoretical B3LYP/6–31G(d,p) quantum mechanical method. The important data for the verification of the present molecular structure quantum mechanical calculations came from the NMR ^1H and ^{13}C measurements of the **ADD**, **7** and **9** spectra. The comparison of the empirical and theoretically



Scheme 4: Possible transformation routes of **ADD (6)** into **7**

predicted chemical shifts is given in Tables 1 and 2. The atom labeling is given in Fig. 2. Tables 1 and 2 clearly show that the theoretically predicted chemical shifts agree well with the experimental data. Therefore, it might be expected that applying the same theoretical methodology will allow to obtain a presumably reasonable geometry and estimation of relative energies for all studied molecules. The energy outputs (Scheme 4, values over the arrows in kcal/mol) were estimated as the energy difference (electronic and nuclear including zero-point vibrations) between the products and substrates. It was assumed that the **ADD** transformation into **7** can follow two routes (R1 and R2): the R1 route (**ADD**-**S1**-**S2**-**7**) through the addition of the pyrrolidine molecule to the C1-C2 double bond with the subsequent elimination of the water molecule after the addition of the second pyrrolidine molecule at the C3 position, and the R2 route

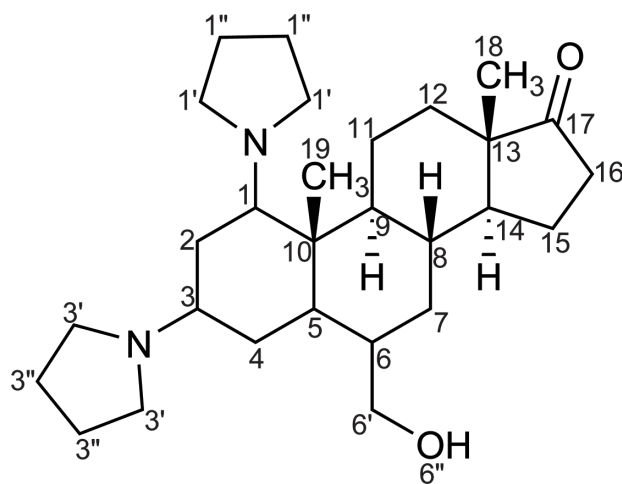


Fig. 2: Atom labeling

Table 1: ^1H NMR chemical shifts (ppm, Kubiszewski et al. 2012) and ^1H chemical shifts predicted with the theoretical B3LYP/6-31G(d,p) method

Atom	ADD	ADD(B3LYP)	9	9 (B3LYP)	7	7 (B3LYP)
1	7.06 d	7.06	6.04 s	6.22	2.98 d	2.97
2	6.23 dd	6.17	6.04 s	6.00	2.26–2.32	2.11
4	6.09 t	6.00	4.79 s	4.43	2.39–2.42	2.50
6	2.40–2.45	2.58	5.22 s	4.94	4.82 s	4.54
	2.49–2.56	2.16			5.03–5.06	4.92
7	1.08–1.19	1.20	1.82–1.91	2.00	1.78–1.84	1.90
	2.06–2.14	1.96	2.23–2.31	2.17	2.20–2.26	2.15
8	1.79–1.85	1.97	1.90–1.98	2.09	1.78–1.84	1.96
9	1.08–1.19	1.24	1.29–1.45	1.52	1.91–1.95	2.40
11	1.66–1.75	1.78	1.46–1.60	1.58	1.38–1.46	1.51
	1.83–1.90	1.77	1.82–1.91	1.70	1.51–1.63	1.57
12	1.23–1.33	1.26	1.29–1.45	1.28	1.30–1.38	1.30
	1.83–1.90	1.88	1.82–1.91	1.85	1.78–1.84	1.84
14	1.23–1.33	1.27	1.29–1.45	1.32	1.38–1.46	1.38
15	1.56–1.65	1.62	1.46–1.60	1.57	1.51–1.63	1.57
	1.94–2.00	1.82	1.82–1.91	1.77	1.93–1.99	1.80
16	2.06–1.14	1.96	2.04–2.13	1.91	2.03–2.12	1.92
	2.44–2.51	2.30	2.41–2.50	2.25	2.40–2.48	2.25
18	0.95 s	0.57	0.92 s	0.48	0.90 s	0.46
		0.96		0.89		0.89
		1.33		1.34		1.35
19	1.27 s	0.66	1.18 s	1.00	1.06 s	0.87
		1.36		1.04		1.10
		1.68		1.41		1.21
1'	–		–		2.35–2.41	1.77
					2.59–2.64	2.15
						2.62
						3.18
1''	–		–		1.51–1.63	1.43
						1.48
						1.75
						1.77
3'	–		3.17 s	3.06	3.11–3.17	3.03
				3.19		3.16
				3.29		3.34
				3.45		3.61
3''	–		1.82–1.91	1.79	1.84–1.91	1.77
				1.80		1.80
				1.80		1.85
				1.85		1.89

(ADD-S3-9-7), starting with the addition of pyrrolidine to the C3 position followed by the formation of **9** and the final addition of the second pyrrolidine leading to **7**. The suggested reaction routes R1 and R2 include the different transformation steps. These appear to be analogous to the known *aza-Michael* addition (Mather et al. 2006) or iminium activated 1,4-addition (Erkkila et al. 2007) of a single amine (here: pyrrolidine) molecule to α,β -unsaturated ketones. The theoretical quantum mechanical calculations of the energy output of the R1 and R2 routes suggest that the pyrrolidine addition to **ADD** can be nearly reversible. The global energy output of the **ADD** to **7** transformation is predicted to be -0.45 kcal/mol only.

The initial reaction of **ADD** with pyrrolidine, according to the quantum mechanical calculations, should favor the R1 route, i.e. the addition of pyrrolidine molecule to the C1-C2 double bond. In fact, the prediction of the specific components in the reaction mixture seems to be problematic because they might exist as a trade-off between some of R1 and R2 reaction steps controlled by different kinetic barriers.

The endothermicity of the ADD to S3 reaction (addition of pyrrolidine at the carbonyl C3 position of **ADD** partly lead-

ing to the formation of impurity **9**) can explain why the elevated temperature of the process should increase the **9** impurity level. A possible role of the acidic catalyst in the ADD transformation has been elucidated with the theoretical model of the protonated **ADD** molecule at the C(3)=O carbonyl moiety, see Fig. 3.

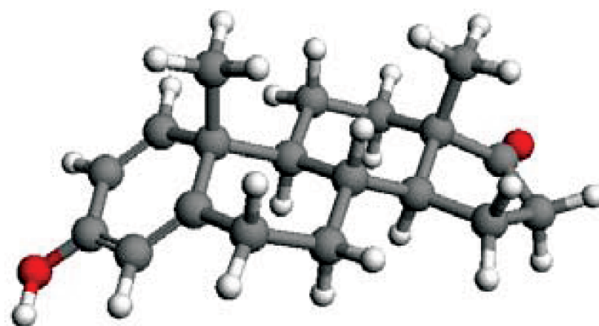


Fig. 3: The **ADD** (**6**) molecule protonated at the C(3)=O carbonyl, according to the B3LYP/6-31G(d,p) theoretical calculations. For artwork the ArgusLab 4.0.1. Mark Thompson and Planaria Software LLC, 2004 was used (freely available <http://www.arguslab.com>)

Table 2: ^{13}C NMR chemical shifts (ppm, Kubiszewski et al. 2012) and ^{13}C chemical shifts predicted with the theoretical B3LYP/6-31G(d,p) method

Atom label	ADD	ADD (B3LYP)	9	9 (B3LYP)	7	7 (B3LYP)
1	155.3	147.6	137.3	134.2	58.3	61.3
2	127.6	125.9	120.1	116.6	22.6	23.7
3	186.1	175.1	139.2	132.5	141.3	133.8
4	124.1	123.1	95.8	94.4	97.9	95.8
5	168.3	160.0	143.4	140.5	142.3	138.2
6	32.5	35.0	116.3	113.0	112.6	110.7
7	32.3	35.1	30.2	33.2	30.9	33.8
8	35.0	37.7	32.6	35.9	31.7	35.0
9	52.3	54.9	44.7	46.9	42.1	44.7
10	43.4	47.0	39.1	44.6	39.3	44.4
11	22.0	24.8	20.5	23.4	19.9	23.5
12	31.2	34.5	31.4	34.6	31.4	34.7
13	47.6	51.1	47.7	50.9	47.7	51.2
14	50.4	52.6	51.9	53.6	51.9	53.8
15	21.9	25.0	21.7	24.8	21.9	25.0
16	35.6	36.8	35.8	37.0	35.9	37.1
17	219.8	210.5	220.9	211.5	221.7	212.0
18	13.8	15.2	13.7	15.1	13.5	15.1
19	18.7	20.6	22.6	24.2	22.6	24.0
1'	–	–	–	–	48.7	46.7
1''	–	–	–	–	23.4	24.4
3'	–	–	47.3	48.3	47.2	47.5
3''	–	–	25.0	27.4	24.7	27.4
				28.0		28.5

The comparison of the calculated natural charges (with the NBO method) of the neutral **ADD** and protonated **ADD** molecules in Table 3 shows that significant changes occur at the C(1) and C(5) carbon atoms. Both carbon atoms adopt partial positive charges that in turn should facilitate the pyrrolidine attack on the C1 position and are likely to activate the C5 region for further transformations.

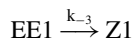
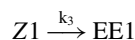
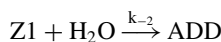
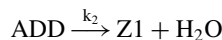
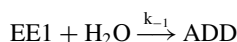
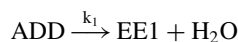
Another modeling has been performed based on the experimental kinetic data.

Table 3: Natural charges, in atomic units, calculated with the B3LYP/6-31G(d,p) method and the NBO method for the **ADD** molecule and its C(3)=O carbonyl-protonated form (Fig. 3). Atom positions according to Fig. 2

Atom / Position	[ADD-H] ⁽⁺⁾	ADD
H O(3)	0.53	–
O C3	–0.60	–0.55
C 3	0.51	0.49
C 4	–0.35	–0.31
C 5	0.20	0.06
C 6	–0.50	–0.48
C 2	–0.31	–0.30
C 1	–0.04	–0.16
C 10	–0.14	–0.11
C 9	–0.22	–0.24
C 19	–0.67	–0.67
H C8	0.27	0.25
H C2	0.29	0.25
H C1	0.27	0.24
H C6	0.28	0.24
O C17	–0.52	–0.54

2.3. Kinetic equations

It is known that the addition reaction tends to follow second-order kinetics based on the concentration of the acceptor and the amine. Taking into account the presence of a large excess of pyrrolidine acting also as a solvent it was assumed that the **ADD** transformation into **7** can be modeled with the mixed first- and second order kinetics. For convenience the following notation was introduced: **EE1**, and **Z1** denote the compounds **7** and **9**, respectively. The models correspond to a simplified versions of the R1 route (**ADD** to **7** directly) and R2 route (**ADD** via **9** to **7**) shown in Scheme 4.



where k 's are the kinetic constants.

Taking into account the mass balance one can obtain the following kinetic equations:

$$\begin{aligned} d[\text{ADD}]/dt = & -(k_1 + k_2) * [\text{ADD}] \\ & + k_{-1} * [\text{EE1}] * [\text{ADD}_0 - \text{ADD}] \\ & + k_{-2} * [\text{ADD}_0 - \text{ADD} - \text{EE1}] \\ & * [\text{ADD}_0 - \text{ADD}] \end{aligned}$$

Table 4a: Time course of the ADD to EE1 (7) transformation without catalyst. Upper value (experiment), lower value (kinetic equations)

Experiment No.	Reaction time (h)	Relative content (%)		
		EE1 7	Z1 9	ADD 6
1	3	8.3	3.8	87.9
		12	5	83
2	20	57.6	11.6	30.8
		58	12	31
3	27	69.8	12.7	17.5
		67	12	21
4	44	76.3	13.4	10.3
		78	13	10
5	48	78.6	12.2	9.2
		79	13	8

Table 4b: Time course of the ADD to EE1 (7) transformation with the catalytic amount of the acetic acid. Upper value (experiment), lower value (kinetic equations)

Experiment No.	Reaction time (h)	Relative content (%)		
		EE1 7	Z1 9	ADD 6
1	1	46	3.5	50.5
		42	3	54
2	2	64	4	32
		65	5	30
3	3	76	4	20
		77	5	17
4	4	83	6	11
		84	5	11
5	5	87	6	7
		88	5	7
6	6	90	5	5
		90	5	5
7	7	92	5	3
		91	5	4
8	24	94	4	2
		94	4	2

$$d[EE1]/dt = k_1 * [ADD] - k_{-1} * [EE1] * [ADD_0 - ADD] + k_3 * [ADD_0 - ADD - EE1] - k_{-3} * [EE1]$$

$$Z1 = ADD_0 - ADD - EE1; \quad H_2O = ADD_0 - ADD$$

$$ADD(0) = ADD_0; \quad EE1(0) = 0$$

We used $ADD(0) = 1.0$ (or 100 %) for reaction modeling. The solution of the above equations corresponds to the time dependence of the relative concentrations of ADD, EE1, Z1 and H_2O species. The kinetic constants were obtained through the application of the least-squares fit to the experimental counterparts at selected time points, establishing model ADD, Z1, and EE1 curves, see Table 4a and Fig. 4 and Table 4b and Fig. 4.

The quasi-Newton method was used for the nonlinear optimization of k -parameters. The optimized values of the kinetic

constants are $k_1 = 0.574$ (0.038); $k_{-1} = 0.000$ (0.003); $k_2 = 0.041$ (0.023), $k_{-2} = 0.376$ (0.000), $k_3 = 0.000$ (0.226), $k_{-3} = 0.015$ (0.035) for the reaction with the acid catalyst while in parentheses there are the values for the reaction without a catalyst. The time dependence of reagents relative concentration with and without the catalyst is shown in the Fig. 4. It is seen that the acid catalyst shortens the reaction time dramatically and this is in turn reflected by the increase of the calculated kinetic constant k_1 . Moreover, a visible reduction of the Z1 impurity content is reflected by the increase of the k_{-2} kinetic constant corresponding to the Z1 annihilation.

3. Experimental

The starting material, i.e. androsta-1,4-diene-3,17-dione (ADD) was purchased from Hangzhou Dayang Chem Co., Ltd. (China). Other chemicals and solvents were purchased from Sigma-Aldrich and used without additional purification. The identity and purity of the obtained compounds were controlled with NMR and HPLC techniques. 1H and ^{13}C NMR spectra were measured on Varian nmrs 600 spectrophotometer at 298K in $CDCl_3$ solutions, using TMS as an internal standard. Two-dimensional techniques: COSY, g-HSQC and g-HMBC were also used for the assignment of signals. HPLC was performed using Waters Alliance apparatus equipped with XDBridge C18 column (150 x 4.5 mm) and PDA (model 2998) detector. De-ionized water pure methanol was used as the mobile phases A and B, respectively. HPLC condition: the flow rate 1.0 mL/min, detection at $\lambda = 247$ nm, the column temperature 45 °C.

3.1. Synthesis of 1 α ,3-di(1-pyrrolidino)androsta-3,5-diene-17-one (7)

The mixture of androsta-1,4-diene-3,17-dione (ADD) (2.5 g, 0.0088 mol), pyrrolidine (7.5 mL) and acetic acid (0.75 mL) was stirred at ambient temperature for 24 h. The sticky reaction mixture was poured into cold water (150 mL). The precipitate was filtered off and washed three times with cold water (3 x 15 mL) then pressed to remove excess water. A water-soaked compound 7 of total yield over 100% was obtained (10 g). The sample of wet, pinkish-orange color product 7 (0.1 g) was immediately dissolved in deuteriochloroform (2 mL), the organic layer was separated and measured in NMR experiments.

The NMR data are shown in Tables 1 and 2.

3.2. Synthesis of 6-(hydroxymethyl)androsta-1,4-diene-3,17-dione (8)

The mixture of androsta-1,4-diene-3,17-dione (ADD) (50.0 g, 0.175 mol), pyrrolidine (150 mL) and acetic acid (15 mL) was stirred at ambient temperature for 24 h. The sticky reaction mixture was dissolved in dichloromethane (250 mL) and washed with water (250 mL). The aqueous layer was additionally extracted with dichloromethane (50 mL) and discarded. The combined organic layers were placed in a flask equipped with a thermometer, stirrer, dropping funnel and a cooling bath. Aqueous 30% formaldehyde (92 mL) was added to the stirred and cooled solution at temperature below 35 °C. Afterwards, the mixture was stirred (300 rpm) for 60 min at ambient temperature, cooled again and 5% sulfuric acid (600 mL) was

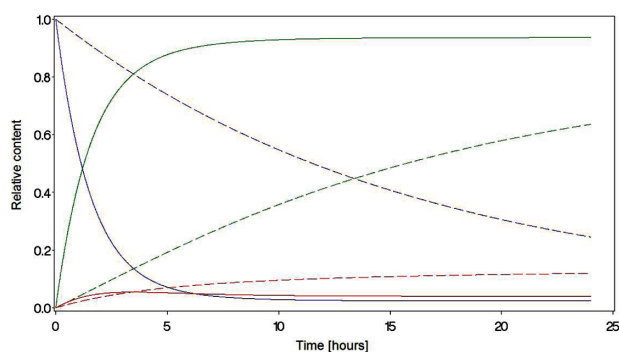


Fig. 4: Solid lines: the relative concentrations of ADD (6, blue), EE1 (7, green) and Z1 (9, red) reagents in the course of the ADD to EE1 transformation with the acetic catalyst, Broken lines: no catalyst applied. The horizontal axis corresponds to the reaction time, in hours

added. The mixture was stirred for 1 min, the organic layer was separated and washed successively with 5% sulfuric acid (50 mL) and 15% brine (3 x 150 mL). The washings were extracted with dichloromethane (100 mL) and discarded. The combined organic layers were placed in a distilling apparatus and about 100 mL of the solvent was distilled off. Then toluene (450 mL) was added to the hot solution and the distillation was carried out again, to distill off 450 mL of the solvents mixture. The suspension was cooled to ambient temperature and stirred for 24 h. The obtained crystals were filtered off, washed with toluene (50 mL) and air dried for 24 h to obtain compound **8**. Yield 43,5 g (79%), purity 97,5% (HPLC).

¹H NMR (δ [ppm]) = 0.96 (s, 3H, -CH₃₍₁₈₎), 1.16–1.22 (m, 1H, CH₍₉₎), 1.24–1.34; 1.87–1.93 (m, 3H, CH₂₍₁₂₎, CH₍₁₄₎), 1.27 (s, 3H, -CH₃₍₁₉₎), 1.30–1.40; 2.08–2.15 (dd, 2H, CH₂₍₇₎), 1.59–1.65; 1.97–2.04 (m, 2H, CH₂₍₁₅₎), 1.65–1.73; 1.87–1.93 (m, 2H, CH₂₍₁₁₎), 1.88–1.96 (m, 1H, CH₍₈₎), 2.08–2.15; 2.45 (m, 2H, CH₂₍₁₆₎), 2.71 (s, 1H, OH), 2.87 (ddd, 1H, CH₍₆₎), 3.86 (ddd, 2H, -CH_{2-O}), 6.20 (s, 1H, =CH₍₄₎), 6.21 (dd, 1H, =CH₍₂₎), 7.05 (d, 1H, =CH₍₁₎).

¹³C NMR (δ [ppm]) = 13.83 (CH₃₍₁₈₎), 19.9 (CH₃₍₁₉₎), 21.6 (CH₂₍₁₁₎), 22.9 (CH₂₍₁₅₎), 31.1 (CH₂₍₁₂₎), 31.2 (CH₍₈₎), 32.4 (CH₂₍₇₎), 35.6 (CH₂₍₁₆₎), 43.5 (C₍₁₀₎), 47.6 (C₍₁₃₎), 48.5 (CH₍₆₎), 50.7 (CH₍₁₄₎), 50.9 (CH₍₉₎), 64.3 (-CH_{2-O}), 126.8 (=CH₍₂₎), 127.7 (=CH₍₄₎), 156.2 (=CH₍₁₎), 167.1 (=C<₍₅₎), 186.1 (>C=O₍₃₎), 220.0 (>C=O₍₁₇₎).

3.3. Synthesis of 3-(1-pyrrolidino)androsta-1,3,5-triene-17-one (**9**)

The mixture of 1 α ,3-dipyrrolidino-androsta-3,5-diene-17-one (**7**) (2.5 g, 0.0088 mol) and *N,N*-dimethylformamide (10 mL) was stirred at reflux to produce a clear solution. Then it was slowly cooled to ambient temperature and stirred for 2 h. The precipitate was filtered off, washed with cold *N,N*-dimethylformamide and dried on air for 72 h, to obtain compound **9**. Yield 1,13 g (55%).

The NMR data are shown in Tables 1 and 2.

3.4. Quantum mechanical calculations

The theoretical quantum mechanical calculations were performed with the density functional B3LYP and the 6–31G(d,p) Gaussian basis set. Total energies corresponded to the local minima and were confirmed by all positive harmonic frequencies. The calculations were performed with the Gaussian G03 and G09 suite of programs.

Acknowledgements: The ICM UW Warsaw University computer center is acknowledged for allocation of computer time and facilities within the grant G18–6. This work was done in a framework of the POIG project UDA-POIG.01.03.01-14-069/08-04

References

Annen K, Hofmeister H, Laurent H, Wiechert R (1982) A simple method for 6-methylation of 3-oxo- Δ^4 -steroids. *Synthesis*: 34–40.

- Bajetta E, Zilembo N, Bichisao E (1999) Aromatase inhibitors in the treatment of postmenopausal breast cancer. *Drugs Aging* 15: 271–283.
- Bonnekessel C, Görlitzer K (2002) Unexpected formation of an estrone-derivative from androsta-1,4-diene-3,17-dione. *Jahrestagung der Deutschen Pharmazeutischen Gesellschaft*, Berlin, 09.-12.10.2002; <http://www.pharmchem.tubs.de/forschung/goerlitzer/dokumente/poster-bonnekessel.pdf>.
- Barton MK (2011) Exemestane is effective for the chemoprevention of breast cancer. *Cancer J Clin* 61: 363–364.
- Buzzetti F, Barbugian N, Lombardi P, DiSalle E (1985) US Pat 4808616.
- Clemett D, Lamb HM (2000) Exemestane: a review of its use in postmenopausal women with advanced breast cancer. *Drugs* 59: 1279–1296.
- Erkkila A, Majander I, Pihko PM (2007) Iminium Catalysis. *Chem Rev* 107: 5416–5470.
- Giudici D, Ornati G, Briatico G, Buzzetti F, Lombardi P, di Salle E (1988) 6-Methylene androsta-1,4-diene-3,17-dione (FCE24304): A new irreversible aromatase inhibitor. *J Steroid Biochem* 30: 391–394.
- Goerlitzer K, Bonnekessel C, Jones PG, Kaufman G (2002) Unexpected formation of an estrone derivative from androsta-1,4-diene-3,17-dione. (in German) *Pharmazie* 57: 808–810.
- Kaczmarek Ł, Cybulski M, Kubiszewski M, Kowalska J, Rosa A (2010) *Pol Pat Appl P-391298*.
- Kubiszewski M, Cybulski M, Kaczmarek Ł (2012) Use of NMR technique to study process and the reaction products in synthesis of Exemestane. (in Polish) *Przem Chem* 91: 272–275.
- Kunnen K, Stehle NW, Weis SW, Pascone JM, Pariza RJ, van Ornum SG (2005) *Pat Appl WO 2005/070951 A1*.
- Lombardi P (2002) Exemestane, a new steroidal aromatase inhibitor of clinical relevance. *Biochim. Biophys. Acta* 1587: 326–337.
- Longo A, Lombardi P (1987) *US Pat 4876045*.
- Mather BD, Viswanathan K, Miller KM, Long TE (2006) Michael addition reactions in macromolecular design for emerging technologies. *Prog Polym Sci* 31: 487–531.
- Miller WR (1990) Endocrine treatment for breast cancers: Biological rationale and current progress. *J Steroid Biochem Mol Biol* 37: 467–480.
- Segaloff A (1978) Hormones and mammary carcinogens. In: McGuire WL (Ed.), *Advances in Research and Treatment, Experimental Biology*, Plenum Press, New York, p. 1–22.
- Wagner H, Ponsold K (1986a) German (East) Pat 258820.
- Wagner H, Ponsold K, Schuman G, (1986b) German (East) Pat 264220.
- Wojciechowska W, Kutner A, Leś A, Szelejewski W (2004) Dehydration of egzo-hydroxymethyl group in androstane derivative; optimization and scale-up. *Pol J Appl Chem* 3–4: 63–74.
- Wojciechowska W (2001) Technological Instruction No. 2843. (unpublished, available in the Pharmaceutical Research Institute).
- World Cancer Report (2008) (Bailey P, Levin B, eds.) Intl Agency for Research on Cancer, Lyon, France; http://www.iarc.fr/en/publications/pdfs-online/wcr/2008/wcr_2008.pdf